Journal of Alloys and Compounds 509 (2011) 2654–2658

Contents lists available at ScienceDirect

Journal of Alloys and Compounds

journal homepage: www.elsevier.com/locate/jallcom

Effect of non-magnetic doping on multi-step magnetization behavior of $Dy_{50-x}Al_xAg_{50}$

H.N. Li[a], Y.Y. Wu[a], G. Cheng[b], Y. Huang[c], S.L. Wang[c], L. Li[c], Z.C. Xia[c,*]

[a] Department of Physics, Huazhong University of Science and Technology,PR China
[b] Department of information Materials Science and Engineering, Guilin University of ElectronicTechonology,PR China
[c] Wuhan National High Magnetic Field Center, Huazhong University of Science and Technology,PR China

ARTICLE INFO

Article history:
Received 20 July 2010
Received in revised form
23 November 2010
Accepted 26 November 2010
Available online 4 December 2010

Keywords:
$Dy_{50-x}Al_xAg_{50}$
Multi-step magnetization
Rotation
Pinning effect

ABSTRACT

The electrical transport and magnetization measurements have been carried out on Al-doped polycrystalline intermetallic compounds $Dy_{50-x}Al_xAg_{50}$ (x = 0, 0.3, 0.6, 1.2, 1.8) in a pulsed high magnetic field, in which multi-step magnetization is observed. Partial substitute of non-magnetic Al^{3+} for Dy^{3+} ions in the compounds increases the critical magnetic fields and the relative area of the magnetic hysteresis loop, which result from the pinning effect, lattice distortion, the change of coupling strength and dilution effect related to the Al^{3+} doping.The experimental results indicate that non-magnetic Al^{3+} ions and induced amorphous phase can pin the rotation and/or growth of magnetic domains, thus, the critical magnetic field can be enhanced by doping non-magnetic ions in the magnetic materials, especially in the permanent magnet materials.

1. Introduction

The rare earth intermetallic compound DyAg has a CsCl-type cubic structure [1]. Much attention has been paid on the magnetic properties of this compound, and it is found that DyAg orders an antiferromagnetic phase and shows three successive magnetic transitions at T_N = 56 K, T_2 = 49 K and T_1 = 46.5 K [2,3]. The magnetic transitions were investigated along [1 0 0], [1 1 0] and [1 1 1] directions of the DyAg single-crystalline sample, where there are multi-step magnetization in all directions [4]. Similar magnetization processes have been observed in the isostructural compound DyCu [5] and the rare-earth-metal tetraboride TbB_4 [6]. The magnetic structure of DyAg was also studied by neutron diffraction [7]. The magnetic properties of non-magnetic ions doped intermetallic antiferromagnet $NdRhIn_5$ were reported [8], and the effect of doping on AFM order, the dilution effect and the crystal field effect were discussed.

In this work, the magnetic properties of polycrystalline intermetallic compounds $Dy_{50-x}Al_xAg_{50}$ (x = 0, 0.3, 0.6, 1.2, 1.8) are investigated in a pulsed high magnetic field. Compared with the single crystalline sample, some abnormal magnetization behaviors are observed in the $Dy_{50-x}Al_xAg_{50}$ polycrystalline samples. Substituting non-magnetic Al^{3+} ions for Dy^{3+} ions shifts the critical magnetic fields to higher magnetic field regions, which may results from the lattice distortion, the change of coupling strength, dilution effect and pinning effect of the doped non-magnetic Al^{3+} ions and induced amorphous phase.

2. Experimental

The polycrystalline samples of $Dy_{50-x}Al_xAg_{50}$ (x = 0, 0.3, 0.6, 1.2, 1.8) were prepared by an arc melting method in high-purity argon atmosphere. High homogeneity of the alloys was ensured by melting the alloy buttons several times using an induction furnace. The obtained rods were annealed under vacuum at 1173 K for 5 days.

The composition and microstructure of the samples were examined by X-ray diffraction (XRD) and Transmission electron microscopy (TEM). The resistance was determined by a four-probe technique. Magnetization measurements, in the temperature range of 15–300 K and up to a maximum field of 30 T, were performed in a pulsed high magnetic field using two concentric pick-up coils connected in series with opposite directions [9]. The pulse field in the shape of one half of a sine wave had peak field up to 50 T at 30 ms pulse duration. Ideally, the voltages induced by the two coils should be entirely compensated without a sample in the coils, but actually they are not completely compensated. Then, two measurements were made: with the sample outside and inside the coils, respectively. The derivatives of magnetization of the sample are obtained from the subtraction of the former signal and the latter one.

3. Results and discussion

The structures of the compounds were investigated with X-ray diffraction and transmission electron microscopy. Fig. 1 shows X-ray diffraction patterns of polycrystalline compounds $Dy_{50-x}Al_xAg_{50}$, where (a), (b), (c), (d) and (e) correspond to x = 0,

* Corresponding author. Tel.: +86 27 87792167 8106; fax: +86 27 87792333.
E-mail address: xia9020@hust.edu.cn (Z.C. Xia).

0925-8388/$ – see front matter © 2010 Elsevier B.V. All rights reserved.
doi:10.1016/j.jallcom.2010.11.182

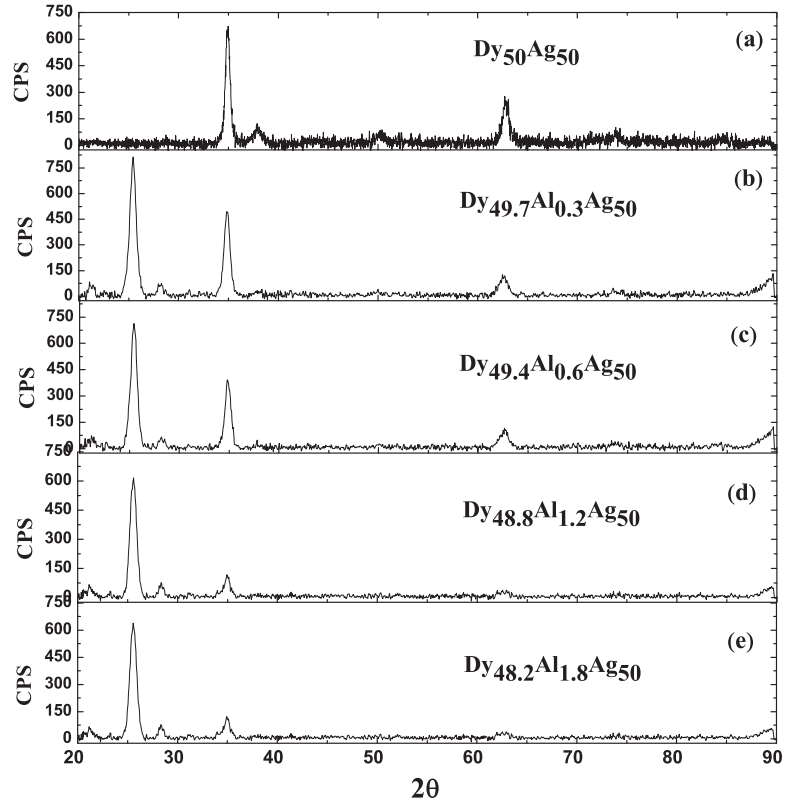

Fig. 1. X-ray diffraction patterns for polycrystalline compounds $Dy_{50-x}Al_xAg_{50}$, (a), (b), (c), (d) and (e) corresponding to $x = 0$, 0.3, 0.6, 1.2, and 1.8, respectively.

0.3, 0.6, 1.2, and 1.8, respectively. Fig. 1(a) shows that the pure $Dy_{50}Ag_{50}$ sample has cubic CsCl-type structure, in which no impurity phases are observed. Compared with the XRD of pure $Dy_{50}Ag_{50}$, the doped compounds $Dy_{50-x}Al_xAg_{50}$ have the similar lattice structure except that a new peak appears, which may indicate non-magnetic Al^{3+} ions and induced amorphous phase interspersed in the matrix. With increasing the doping level, the amorphous phase increases gradually. Fig. 2(a) (b), (c) and (d) show the TEM micrographs of polycrystalline compounds $Dy_{50-x}Al_xAg_{50}$ with $x = 0.3$, $x = 0.6$, $x = 1.2$ and $x = 1.8$, respectively. In Fig. 2(a), the new phase

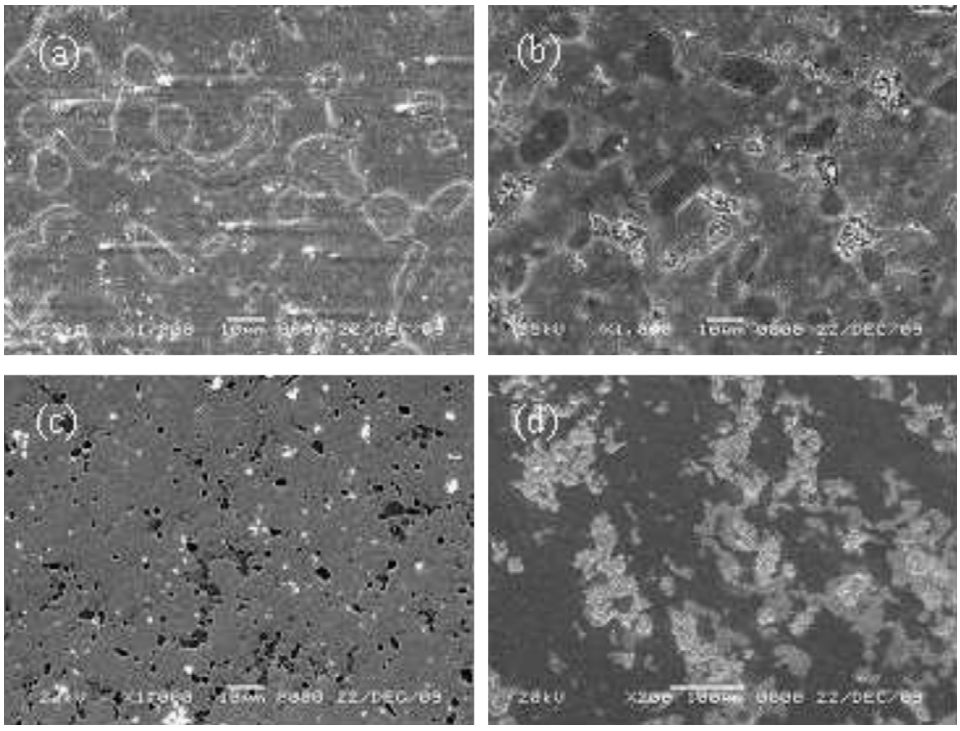

Fig. 2. TEM micrographs of polycrystalline intermetallic compounds $Dy_{50-x}Al_xAg_{50}$. (a) $x = 0.3$, (b) $x = 0.6$, (c) $x = 1.2$, (d) $x = 1.8$.

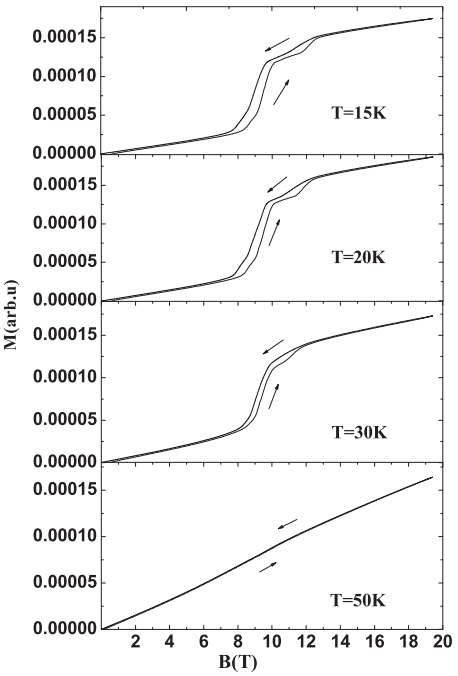

Fig. 3. Magnetic field dependence of magnetization of $Dy_{50}Ag_{50}$ measured at different temperatures.

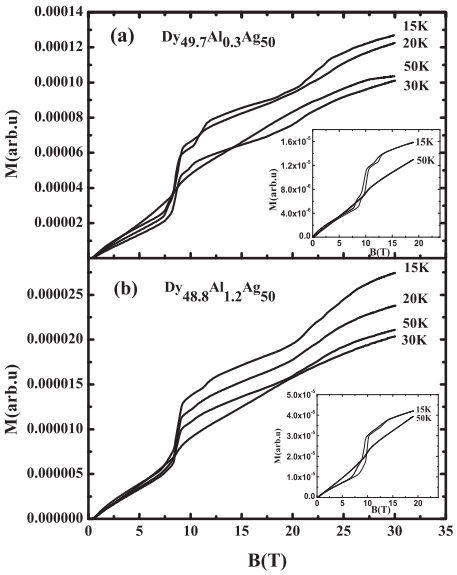

Fig. 4. Magnetic field dependence of magnetization of $Dy_{50-x}Al_xAg_{50}$ at different temperatures and doping level, (a) $x = 0.3$, (b) $x = 1.2$. The insets are the hysteresis loops measured at 15 K and 50 K.

appears which correspond to the new diffraction peak observed in $Dy_{49.7}Al_{0.3}Ag_{50}$. Analysis of Fig. 1(c)–(e), the peak of new phase increases with the doping level of Al^{3+} ions. Correspondingly, the non-magnetic Al^{3+} ions and induced amorphous phase becomes more obvious as shown in Fig. 2(b)–(d).

The temperature dependence of resistance of $Dy_{50-x}Al_xAg_{50}$ was measured (not shown in this paper). For pure compound, the transition temperature of ferromagnetic phase to antiferromagnetic phase is $T_N = 48$ K, which is slightly different from the reported temperatures 55 K [10] and 56.7 K [2]. Meanwhile, another obvious difference is that a plateau appears in the polycrystalline compound between 48 K and 55 K. According to the neutron diffraction data [5], the plateau may correspond to a balance of different magnetic structures. Another possible reason is that the grain boundary plays an important role in the formation of the plateau, which balances the effect of the inner thermal fluctuation. For the doped compounds with $x = 0.3$ and $x = 0.6$, T_N is 56 K and 60 K, respectively. These results suggest the ferromagnetic–antiferromagnetic phase transition temperature increases as the doping level increase, which is different from the intermetallic antiferromagnet $NdRhIn_5$ [8] and Sn doped Mn–Ni–Ga alloys [11].

Fig. 3 shows the isothermal magnetization behavior of $Dy_{50}Ag_{50}$ in a pulsed high magnetic field (up to 19 T) at different temperatures. The data were collected while the magnetic field sweeping in 30 ms. In these measurements, an arbitrary unit is used to characterize the relative value of the magnetization; the absolute value of the magnetization is not accurate due to deviations of the sample position inside the pick-up coils in different measurements. As shown in Fig. 3(a), at 15 K, two-steps transition is observed at the magnetic fields of 8 T and 11.6 T, which is similar to the magnetization curve of single crystal DyAg in a pulsed magnetic field up to 30 T at 4.2 K [12]. These field-induced transitions are related to spin reorientation during the magnetization process. With decreasing the magnetic field, the demagnetization process follows the virgin curve closely until about 12.5 T, where the first transition occurs, then the magnetization gradually decreases and shows a sharp fall at about 9.7 T, and the curve merges with the virgin one again. In the magnetization curve, a hysteresis loop is observed in the intermediate magnetic field range. At 20 K, as shown in Fig. 3(b), except that the critical magnetic fields become higher, similar transitions appear just as that observed at 15 K. This result is different from the situation of Gd_5Ge_4 [13]. The higher critical field may due to the larger thermal fluctuations of the inner atoms at higher temperatures. At 30 K, the magnetization curve is also similar to that observed at 15 K and 20 K, in addition, the critical magnetic fields become much higher; another obvious difference is that the hysteresis loop becomes narrower than that observed at 15 K and 20 K. This may indicate that the influence of thermal fluctuation is larger than that of the pinning effect in this higher temperature region. As shown in Fig. 3(d), the hysteresis loop and the transition steps almost disappear when the temperature increases to 50 K, which indicate a transition from one type of magnetic structure (AF1) to another one (AF2) [2]. The details of magnetization processes may be described as follows: at the beginning of measurements, the sample is in antiferromagnetic phase below 48 K. With increasing the magnetic field, multi-step magnetizations were observed, implying a field-induced ferromagnetic alignment (AFM to FM transition). Meanwhile, these magnetization processes depend mainly on the competitions of the pinning effect, the Lorentz force and the thermal fluctuation.

In order to investigate the effect of doping level on magnetic behaviors of the intermetallic compounds, non-magnetic ions are introduced into the lattice structure by partially substituting Al^{3+} ions for Dy^{3+} ions. The magnetization curves for $x = 0.3$ and $x = 1.2$ are shown in Fig. 4. In low magnetic field region, these doped compounds have similar magnetization behaviors with the pure $Dy_{50}Ag_{50}$. However, in higher magnetic field region, for different doping level, the field-induced transition is different. For $x = 0.3$, magnetization behaviors of different temperatures are shown in Fig. 4(a). At $T = 15$ K, several magnetization steps are observed, indicating the rearrangement of the spin configuration in the compound. With increasing the temperature, the transition steps disappear, and almost a linear magnetization behavior is observed at 50 K. For $x = 1.2$, multi-step magnetization becomes not obvious. However, a small step transition is observed for $x = 1.2$ at 50 K, which suggests that an antiferromagnetic phase still exists in the doped compound at 50 K. As shown in the inset of Fig. 4, with increasing the doping level, the relative area of the hysteresis loop increases. These results suggest that partial substitute non-

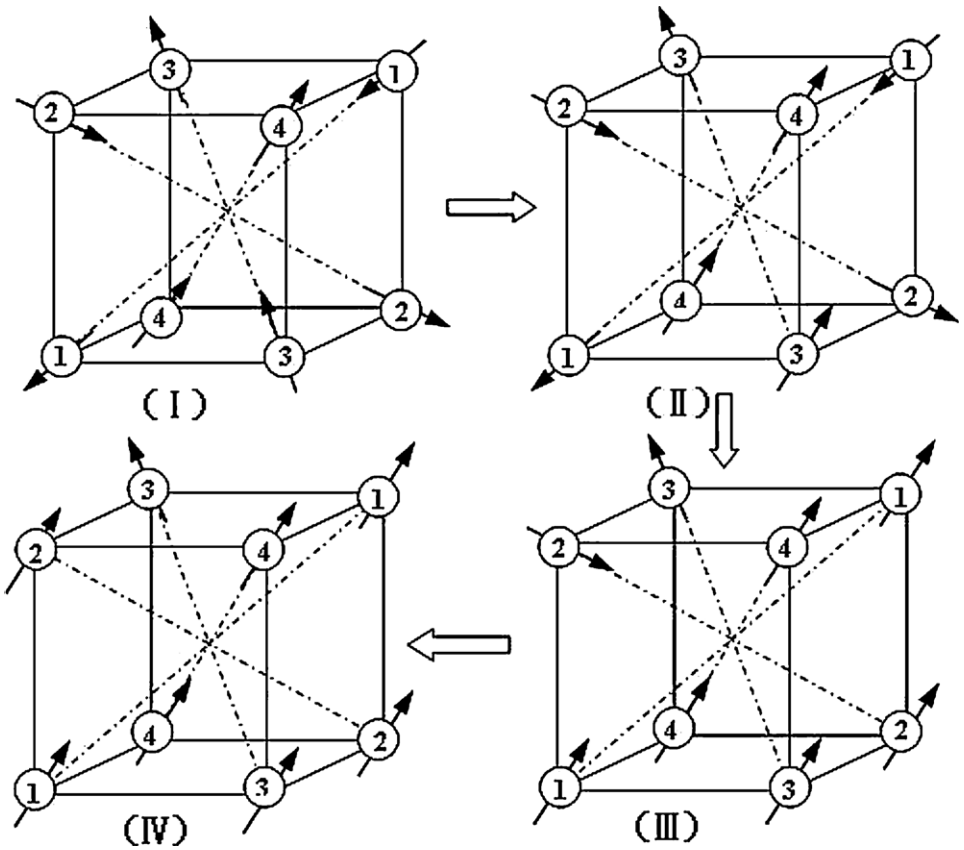

Fig. 5. The possible spin structures of $Dy_{50}Ag_{50}$ at 20 K and in different applied magnetic field. The arrows show the directions of the magnetic moments.

magnetic Al^{3+} ions induce the amorphous phase appears and have pinning effect on the spin reorientation.

As studied by neutron diffraction, for a single crystal sample, between T_N and T_2, the magnetic structure is an incommensurate state characterized by the $(1/2 \pm \tau, 1/2 \pm \tau, 0)$ propagation vector with $\tau = 0.0473$, and it seems to adopt a double-q structure [3]. Below T_1, the magnetic structure is of $(\pi, \pi, 0)$ symmetry with a triple-q structure and the spins are aligned along the four equivalent [1 1 1] directions [3], and a unique model of magnetic structure of pure DyAg was reported [5]. The properties of magnetization has been investigated in high magnetic fields along the [1 0 0], [0 1 0] and [1 1 1] axis in a single crystal sample [4]. Here, we analyze the formation of each step in the magnetization process as following. According to Ref. [4], each step corresponds to a spin reorientation. Fig. 5 shows the possible spin structure of $Dy_{50}Ag_{50}$ at $T = 20$ K, where state (I) shows the ground state. As shown in state (II), the first magnetization step may correspond to an atom, located at the vertex of cubic structure, reorients to the direction of the applied magnetic field. For the middle multi-step magnetization process, which observed in Fig. 3 ($T = 20$ K), corresponds to the spin reorientation of the three atoms, which located at the [1 0 0], [1 1 0] and [1 1 1] axis as show in state (III). Compare with the easy axis [1 1 1], the magnetizations of the sample along the [1 0 0], [1 1 0] axes are more difficult, which leads to the magnetization steps occur at different magnetic fields. The last step corresponds to the transition from state (III) to the spin reorientation as show in (IV). Meanwhile, different magnetization steps have different slope, which may result from the different angles of the three axes with the applied magnetic field. However, these spin structures of $Dy_{50}Ag_{50}$ polycrystalline are not clear due to the grain boundaries, which should be intrinsic barriers for spin reorientation. Fig. 6 shows the doping level x dependence of critical fields H_{c1}, H_{c2}, H_{c3} and H_{c4}. At 15 K, with increasing the doping level x, the critical magnetic fields increase, suggesting that the amorphous phase which induced by doped non-magnetic Al^{3+} ions have pinning effect on the spin reorientation in a pulsed magnetic field. Meanwhile, a new transition (H_{c4}) is observed in both the pure and the lower doping level samples. At 50 K, as shown in the inset of Fig. 6, with increasing the doping level, the critical magnetic field H_{c1} increases.

Compared with the pure $Dy_{50}Ag_{50}$, different magnetization behaviors observed in the doped samples of $Dy_{50-x}Al_xAg_{50}$ ($x = 0.3$, 0.6, 1.2, 1.8) may be understood as following: (1) The amorphous phase which induced by doped non-magnetic Al^{3+} ions have pin-

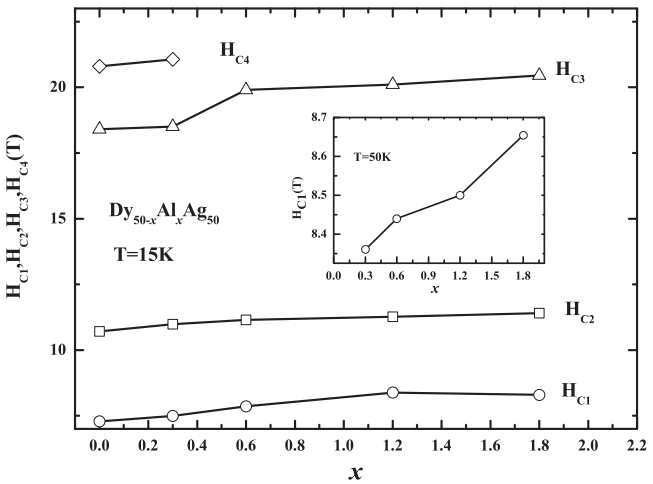

Fig. 6. Doping level x dependence of critical fields H_{c1}, H_{c2}, H_{c3} and H_{c4}.The inset is the doping level x dependence of H_{c1} measured at 50 K.

ning effect on the rotation and/or growth of FM domains in the magnetization process, leads to the high critical magnetic fields and large hysteresis loops. (2) Partially substituting non-magnetic Al^{3+} ions for Dy^{3+} induces the cubic CsCl-type structure distortion due to the different ion radius, in which the ion radius of Dy^{3+} and Al^{3+} are 0.91 Åand 0.51 Å respectively. (3) Dilution effect is also considered. Partially substituting non-magnetic Al^{3+} ions for Dy^{3+} ions dilutes the magnetic interaction between Dy^{3+} ions, thus, suppresses the magnetic coupling between Dy^{3+}ions and leads to higher critical fields as shown in Fig. 6. However, there is a non-linear relation between the critical fields and the doping level; this indicates the complex effects of the non-magnetic doping on the magnetization process of intermetallic alloys.

4. Conclusions

In this paper, we have discussed the low temperature magnetization of non-magnetic Al^{3+} ions doped polycrystalline intermetallic compounds $Dy_{50-x}Al_xAg_{50}$ ($x = 0$, 0.3, 0.6, 1.2, 1.8). With increasing the doping level of Al^{3+} ions, the amorphous phase segregates obviously and the critical field increases. Experimental results reveal that the pinning effect which from the appearances of the amorphous phase plays an important role on the magnetization process, meanwhile, lattice distortion and dilution effect are also included. Compared with the single crystal sample, the multi-step magnetization of the polycrystalline sample is more sensitive to the temperature and magnetic field. Especially, the critical magnetic fields can be increased by doping non-magnetic ions in the intermetallic alloys.

References

[1] J.R. Mignod, J. Phys. Colloques 40 (1979), C5-95–C5-100.
[2] T. Kaneko, H. Yoshida, M. Ohashi, S. Abe, J. Magn. Magn. Mater. 70 (1987) 277–278.
[3] P. Morin, J. Rouchy, K. Yonenobu, A. Yamagishi, M. Date, J. Magn. Magn. Mater. 81 (1989) 247–258.
[4] S. Yoshii, K. Kindo, H. Nakanishi, T. Kakeshita, Phys. B 346 (2004) 160–164.
[5] I. Kakeya, T. Kakeshita, K. Kindo, Y. Yamamoto, T. Saburi, J. Phys. Soc. Jpn. 68 (1999) 1025–1030.
[6] S. Yoshii, T. Yamanoto, M. Hagiwara, S. Michimura, A. Shigekawa, F. Iga, T. Takabatake, K. Kindo, Phys. Rev. Lett. 101 (2008) 087202.
[7] K. Ubukata, M. Arai, M. Fujita, M. Mino, T. Bokui, P. Morin, M. Motokawa, Phys. B 213–214 (1995) 1022–1024.
[8] R. Lora-Serrano, D.J. Garcia, E. Miranda, C. Adriano, L. Bufaical, J.G.S. Duque, P.G. Pagliuso, Phys. B 404 (2009) 3059–3062.
[9] R. Grössinger, J. Alloys Compd. 369 (2004) 5–9.
[10] F. Canepa, F. Merio, A. Palenzona, J. Phys. Condens. Mater. 1 (1989) 1429–1436.
[11] Z.Y. Gao, C. Liu, D. Wu, W.J. Zhang, W. Cai, J. Magn. Magn. Mater. 322 (2010) 2488–2492.
[12] S. Miura, T. Kaneko, S. Abe, G. Kido, H. Yoshida, K. Kamigaki, Y. Nakagawa, J. Phys. Colloques 49 (1988), C8-393–C8-394.
[13] Z.W. Ouyang, H. Nojiri, S. Yoshii, G.H. Rao, Y.C. Wang, V.K. Pecharsky, K.A. Gschneidner, Phys. Rev. B 77 (2008) 184426.